Progress In Electromagnetics Research, PIER 102, 181–195, 2010

A TDIE/TDPO HYBRID METHOD FOR THE ANALYSIS OF TM TRANSIENT SCATTERING FROM TWO-DIMENSIONAL COMBINATIVE CONDUCTING CYLINDERS

S.-T. Qin, S.-X. Gong, R. Wang, and L.-X. Guo

School of Electronic Engineering
Xidian University
No. 2, Taibai Road, Xi'an City, Shaanxi Province, China

Abstract—In this work, a hybrid method which combines time domain integral equation method (TDIE) with time domain physical optics method (TDPO) is presented for the problem of TM transient scattering from two-dimensional (2-D) combinative conducting targets. The explicit solution of Marching-On-in-Time (MOT) is developed. The high accuracy and efficiency of this hybrid method are demonstrated by comparing the numerical results of this hybrid method with those obtained by TDIE. To obtain 2-D transient far scattered field, a concise algorithm about time-domain near-zone to far-zone transformation without double Fourier transform is presented for TDIE and hybrid method, and its numerical results are verified by comparing with the results obtained from inverse discrete Fourier transform (IDFT) techniques.

1. INTRODUCTION

Integral equation (IE) is widely used for the numerical analysis of electromagnetic radiation and scattering [1–14]. Especially the time domain integral equation (TDIE) has been receiving much interest in studying many practical transient electromagnetic problems [15–19]. This is because there has been an increasing interest in short pulse radar design for high resolution and target identification problems. However, for electrically large objects, TDIE suffers great difficulties. Thus, it is necessary to develop fast algorithm for TDIE. So far, there are two kinds of fast algorithm based on TDIE: one is the plane

Corresponding author: R. Wang (doufuruier@yahoo.cn).

wave time-domain algorithm (PWTD) [20–22] proposed by Shanker et al., which is actually the time-domain version of fast multi-pole method (FMM) [8–10]. This method could decrease computational complexity significantly, but the method itself is very complex and not easy to program. Another one is the hybrid method which combines TDIE with time domain physical optics method (TDPO) [23–25]. The interactions of the currents in TDPO region are neglected in this method. Therefore, computational complexity is reduced greatly. Compared to PWTD the hybrid method of TDIE/TDPO is also very accurate [24] and easy to program, hence is a very potential fast method for transient EM scattering problems. However, all the published works about this hybrid method only involved in 3-D structure [23–25] even though the hybrid method for 2-D case is very different from that for 3-D case.

In this paper, the TDIE/TDPO hybrid method is extended to the problem of transient scattering from 2-D combinative conducting targets in TM case. The combinative targets consist of two cylinders: electrically large but smooth one (modeled as TDPO region) and electrically small but complicated one (modeled as TDIE region). The field strength in TDIE is regarded as the contributions of the currents in both TDIE and TDPO regions while the field strength in TDPO is regarded only as the contributions of those on TDIE. The interactions of the currents in TDPO region are neglected. Based on above consideration, by using time-domain electric field integral equation (EFIE), the explicit MOT is developed in detail. Numerical results are compared with those obtained by TDIE, and a good agreement is achieved.

Traditional method for computing 2-D transient far scattered field needs double Fourier transform [30], which is very complex, and most references about 2-D TDIE have not mentioned the calculations of transient far scattered field [26–29]. In this paper, a concise time-domain near-zone to far-zone transformation algorithm without double Fourier transform is presented, and the numerical results are verified by comparing with those obtained from IDFT.

2. THEORY AND FORMULATION

2.1. Time-domain Electric Field Integral Equation (TD-EFIE)

Let infinite conducting cylinders parallel to the z-axis, and C denotes the cross section of the cylinder. For TM incident case, the current is only z directed and does not vary with z. Therefore, following TD-

EFIE may be derived [29]:

$$\left[\vec{E}^{\text{inc}}(\vec{\rho},t)\right]_{\tan} = \left[\frac{\partial \vec{A}(\vec{\rho},t)}{\partial t}\right]_{\tan} \tag{1}$$

where subscript tan refers to the tangential component along the length of the cylinder. $\vec{E}^{inc}$ is the incident electric field, and $\vec{A}$ is the magnetic vector potentials which may be expressed as:

$$\vec{A}(\vec{\rho},t) = \frac{\mu}{4\pi}\int_C \int_{z'=-\infty}^{+\infty} \frac{1}{R}\vec{J}\left(\vec{\rho}',t-\frac{R}{c}\right) dC'dz' \tag{2}$$

where μ is the permeability of the surrounding medium, and c is the velocity of propagation of electromagnetic wave. $R = \sqrt{|\vec{\rho}-\vec{\rho}'|^2+z'^2}$ is the distance from the field point $\vec{\rho}$ to the source point $(\vec{\rho}', z')$.

By integrating both sides of Eq. (1) with respect to time, we obtain:

$$\vec{A}_{\tan}(\vec{\rho},t) = \int_0^t \vec{E}^{\text{inc}}_{\tan}(\vec{\rho},t)dt \tag{3}$$

2.2. Discretization Scheme for Combinative Cylinders

As discussed in Section 1, for combinative cylinders, electrically large/smooth one is modeled as TDPO region, while electrically small one is modeled as TDIE region, and two cylinders are separate, as shown in Fig. 1.

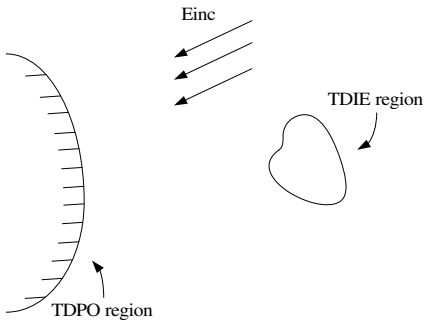

Figure 1. Regions for TDIE and TDPO.

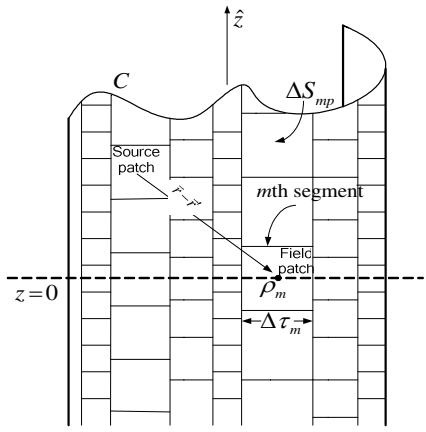

Figure 2. The grid scheme.

For both TDIE and TDPO regions, we use the grid scheme proposed in [26–29], in which square patches were used. As shown in Fig. 2, we first approximate the contour C into straight-line segments, each of length $\Delta\tau_m$. Then, we divide the whole mth column, i.e., from $(-\infty < z < \infty)$ associated with linear segment m, into zones with $\Delta z = \Delta\tau_m$ to obtain a square grid. Note that the patch heights from one column to another may be different. Because the cylinders are infinite along the z-axis, all the field quantities are invariant with respect to the z variable. Hence, for simplicity, the currents observed will be restricted at $z = 0$.

2.3. Explicit MOT Solution Procedure

A set of basis functions for expansion purposes is defined as follows [29]:

$$j_m(\vec{\rho}) = \begin{cases} 1 & \vec{\rho} \in m\text{th segment} \\ 0 & \text{else} \end{cases} \tag{4}$$

Testing functions are similar to basis functions, and the inner product is defined as:

$$\left\langle \vec{a}, \vec{b} \right\rangle = \int_S \vec{a} \cdot \vec{b}\, ds \tag{5}$$

Let the number of the linear segments of TDIE and TDPO regions be N, K respectively, and let

$$\vec{J}_{\text{TDIE}}(\vec{\rho}, t) = \hat{z} \sum\nolimits_{n=1}^{N} I_n(t) j_n(\vec{\rho}) \tag{6}$$

$$\vec{J}_{\text{TDPO}}(\vec{\rho}, t) = \hat{z} \sum\nolimits_{k=1}^{K} I_k(t) j_k(\vec{\rho}) \tag{7}$$

where $\hat{z}$ represents the unit vector along z-axis, and $I_n(t)$, $I_k(t)$ are the unknown coefficients at the nth segment of TDIE region and the kth segment of TDPO region, respectively. As described in Section 1, for TDIE region, in each time step, we apply the method of moments (MOM) to test Eq. (3) [29]:

$$\left\langle \hat{z} j_m, \vec{A}(\vec{\rho}, t) \right\rangle = \left\langle \hat{z} j_m, \int_0^t \vec{E}^{\text{inc}}(\vec{\rho}, t) dt \right\rangle \tag{8}$$

Approximately, assuming that $\vec{A}(\vec{\rho}, t)$ does not vary within the mth segment, we obtain:

$$\vec{A}(\vec{\rho}_m, t) = \int_0^t \vec{E}^{\text{inc}}(\vec{\rho}_m, \tau) d\tau \tag{9}$$

where $\vec{\rho}_m$ is the middle point of the mth segment of TDIE region. Now we calculate $\vec{A}(\vec{\rho}_m, t)$, which is regarded as the contributions of the currents both in TDIE and TDPO regions:

$$\vec{A}(\vec{\rho}_m, t) = \frac{\hat{z}\mu}{4\pi} \int_{C_{\text{TDIE}}} \int_{z'=-\infty}^{\infty} \frac{\sum_{n=1}^{N} I_n(t - R_m/c) j_n(\vec{\rho}')}{R_m} dz' dC'$$
$$+ \frac{\hat{z}\mu}{4\pi} \int_{C_{\text{TDPO}}} \int_{z'=-\infty}^{\infty} \frac{\sum_{k=1}^{K} I_k(t - R_m/c) j_k(\vec{\rho}')}{R_m} dz' dC'$$
$$\approx \frac{\hat{z}\mu}{4\pi} \sum_{n=1}^{N} \sum_{p=-\infty}^{\infty} I_n\left(t - \frac{R_{mnp}}{c}\right) F_{mnp} + \frac{\hat{z}\mu}{4\pi} \sum_{k=1}^{K} \sum_{p=-\infty}^{\infty} I_k\left(t - \frac{R_{mkp}}{c}\right) F_{mkp} \quad (10)$$

where

$$F_{mnp} = \int_{\Delta S_{np}} \frac{1}{R_m} ds' \text{ and } F_{mkp} = \int_{\Delta S_{kp}} \frac{1}{R_m} ds' \quad (11)$$

$$R_m = \sqrt{|\vec{\rho}_m - \vec{\rho}'|^2 + z'^2} \quad (12)$$

$$R_{mnp} = \sqrt{|\vec{\rho}_m - \vec{\rho}'_n|^2 + (p\Delta\tau_n)^2} \text{ and } R_{mkp} = \sqrt{|\vec{\rho}_m - \vec{\rho}'_k|^2 + (p\Delta\tau_k)^2} \quad (13)$$

In Eqs. (10)–(13), $\vec{\rho}_m$, $\vec{\rho}'_n$, $\vec{\rho}'_k$ represent the middle point of the mth, nth segments of TDIE region and the kth segment of TDPO region, respectively. $\Delta\tau_n$ and $\Delta\tau_k$ represent the lengths of the nth and kth square patches, and p represents the ordinal number of the square patch along the z-axis and from $z = 0$. ΔS_{np} represents the pth patch of the nth segment in TDIE region along the z-axis. Similarly, ΔS_{kp} represents the patch in TDPO region.

For non-self terms, i.e., where $\vec{r}$ and $\vec{r}'$ do not belong to the same patch, the $1/R$ integral may be approximated by the patch area divided by the distance between the patch centers. For self terms, the integration may be carried out analytically [29]. Then the values of F_{mnp} can be given by:

$$F_{mnp} = \begin{cases} \frac{(\Delta\tau_n)^2}{\sqrt{|\vec{\rho}_m - \vec{\rho}'_n|^2 + (p\Delta\tau_n)^2}} & m \neq 0 \text{ or } p \neq 0 \\ 4\Delta\tau_n \ln(1 + \sqrt{2}) & m = n \text{ and } p = 0 \end{cases} \quad (14)$$

It should be noted that the field point is only in TDIE region, and for the source point of TDPO region, it is impossible that $\vec{r}$ and $\vec{r}'$ belong to the same patch. Thus F_{mkp} can be given by:

$$F_{mkp} = \frac{(\Delta\tau_k)^2}{\sqrt{|\vec{\rho}_m - \vec{\rho}'_k|^2 + (p\Delta\tau_k)^2}} \quad (15)$$

Next, we deal with the calculation of $I_k(t)$. As discussed in Section 1, for TDPO region, the interactions of the currents are neglected, and the induced currents are produced in two ways: one is the contribution of the incident wave, and the other is the contribution of the currents of TDIE region. Thus $\vec{J}_{\text{TDPO}}$ can be given by [24]:

$$\vec{J}_{\text{TDPO}}(\vec{\rho},t) = 2\hat{k} \times \vec{H}^{inc}(\vec{\rho},t) + 2\hat{k} \times \vec{H}_S(\vec{\rho},t) \tag{16}$$

where $\hat{k}$ is the outward-directed unit vector normal to the contour C, and $\vec{H}_S$ is the scattered field produced by $\vec{J}_{\text{TDIE}}$. $\vec{H}^{inc}$ is the incident magnetic field and is defined as $\vec{H}^{inc} = (1/\eta)\hat{k}^{inc} \times \vec{E}^{inc}$, where η is the wave impedance of the surrounding medium, and $\hat{k}^{inc}$ is the unit vector in the direction of propagation of the incident wave. $\vec{H}_S$ can be expressed as:

$$\begin{aligned}\vec{H}_S(\vec{\rho},t) &= \frac{1}{\mu}\nabla\times\vec{A}_S = \nabla\times\int_{C_{\text{TDIE}}}\int_{z'=-\infty}^{\infty}\frac{\hat{z}\sum_{n=1}^{N} I_n(t-R/c)j_n(\vec{\rho}')}{4\pi R}dz'dl' \\ &= \nabla\times\sum_{n=1}^{N}\sum_{p=-\infty}^{\infty}\frac{\hat{z}I_n(t-R_{np}/c)(\Delta\tau_n)^2}{4\pi R_{np}}\end{aligned} \tag{17}$$

where

$$R = \sqrt{|\vec{\rho}-\vec{\rho}'|^2 + z'^2} \text{ and } R_{np} = \sqrt{|\vec{\rho}-\vec{\rho}_n'|^2 + (p\Delta\tau_n)^2} \tag{18}$$

Noting that the right side of Eq. (17) is expressed as the rotation of the product of a vector and a scalar, so by using the formula of rotation operation $\nabla \times (\vec{a}f) = f(\nabla \times \vec{a}) - \vec{a}\nabla f$ and $\nabla \times \hat{z} = 0$, we get:

$$\begin{aligned}\vec{H}_S(\vec{\rho},t) = -\hat{z}\times\sum_{n=1}^{N}\sum_{p=-\infty}^{\infty}\nabla\left[\frac{I_n(t-R_{np}/c)(\Delta\tau_n)^2}{4\pi R_{np}}\right] = -\frac{\hat{z}}{4\pi}\times\sum_{n=1}^{N}\sum_{p=-\infty}^{\infty} \\ \left[\frac{(\Delta\tau_n)^2\nabla I_n(t-R_{np}/c)}{R_{np}} + (\Delta\tau_n)^2 I_n(t-R_{np}/c)\nabla\left(\frac{1}{R_{np}}\right)\right]\end{aligned} \tag{19}$$

Using simple algebra:

$$\nabla I_n\left(t-\frac{R_{np}}{c}\right) = -\frac{1}{c}\hat{R}_{np}\frac{\partial I_n(t_R)}{\partial t_R} \text{ and } \nabla\left(\frac{1}{R_{np}}\right) = -\hat{R}_{np}\frac{1}{(R_{np})^2} \tag{20}$$

where $\hat{R}_{np}$ represents the unit vector in the direction from the source point (TDIE region) to the observation point (TDPO region), and $t_R = t - R_{np}/c$. Combining Eqs. (19) and (20) gives:

$$\vec{H}_S(\vec{\rho},t) = \sum_{n=1}^{N}\sum_{p=-\infty}^{\infty}\frac{\hat{z}\times\hat{R}_{np}}{4\pi}\left[\frac{(\Delta\tau_n)^2}{cR_{np}}\frac{\partial I_n(t_R)}{\partial t_R} + \frac{(\Delta\tau_n)^2}{(R_{np})^2}I_n\left(t-\frac{R_{np}}{c}\right)\right] \tag{21}$$

Combining Eqs. (7), (16) and (21) gives:

$$I_k(t) = 2\hat{k} \times \vec{H}^{inc}(\vec{\rho}_k, t) \cdot \hat{z} + \sum_{n=1}^{N} (\Delta\tau_n)^2 \sum_{p=-\infty}^{\infty} \frac{\hat{k} \cdot \hat{R}_{knp}}{2\pi R_{knp}} \left[\frac{1}{c} \frac{\partial I_n(t_R)}{\partial t_R} + \frac{1}{R_{knp}} I_n \left(t - \frac{R_{knp}}{c} \right) \right] \quad (22)$$

where $I_k(t)$ is the unknown coefficients at the kth segment in TDPO region. The time derivative of the current is approximated with a center finite difference as:

$$\frac{\partial I_n(t_R)}{\partial t_R} = \frac{I_n(t + 0.5\Delta t - R_{knp}/c) - I_n(t - 0.5\Delta t - R_{knp}/c)}{\Delta t} \quad (23)$$

Equation (22) shows that $I_k(t)$ in TDPO region is determined by the incident fields and scattered fields from the currents in TDIE region. Now we consider the calculation of $I_n(t)$ in TDIE region. If the time step Δt meets Courant criterion, $c\Delta t < \Delta R_{\min}/\sqrt{2}$, where $R_{\min}$ is the minimum distance between patch centers. It is obvious that $t_i - R/c < t_{i-1}$ unless $m = n$ and $p = 0$, then we obtain:

$$\vec{A}(\vec{\rho}_m, t_i) = \frac{\hat{z}\mu}{4\pi} F_{mm0} I_m(t_i) + \frac{\hat{z}\mu}{4\pi} \sum_{\substack{n=1 \\ m \neq n}}^{N} \sum_{\substack{p=-\infty \\ \text{or } p \neq 0}}^{\infty} I_n \left(t_i - \frac{R_{mnp}}{c} \right) F_{mnp} + \frac{\hat{z}\mu}{4\pi} \sum_{k=1}^{K} \sum_{p=-\infty}^{\infty} I_k \left(t_i - \frac{R_{mkp}}{c} \right) F_{mkp} \quad (24)$$

Let $B(\vec{\rho}_m, t_i)$ denote the second term of the right-hand side in Eq. (24) and $C(\vec{\rho}_m, t_i)$ the third term, and by combining Eqs. (24) and (9) we can obtain:

$$\frac{\mu}{4\pi} F_{mm0} I_m(t_i) = \int_0^{t_i} E^{\text{inc}}(\vec{\rho}, \tau) d\tau - B(\vec{\rho}_m, t_i) - C(\vec{\rho}_m, t_i) \quad (25)$$

Obviously, the left-hand side in Eq. (25) involves term only at $t = t_i$, whereas the right-hand side contains the terms for $t \leq t_{i-1}$. Hence, all $I_m(t_i)$ in TDIE region can be obtained from Eq. (25) by using $I(t_{i-1})$ and all previous currents of both TDIE and TDPO regions. Then, $I_k(t_i)$ of TDPO region can be obtained from Eq. (22) by using $I_m(t_i)$ in TDIE region as well as the incident field. This method needs no matrix inversion and is an explicit method.

In order to avoid the late time instability, a three-step averaging technique is adopted [29], which simply approximates the averaged values $\tilde{I}_m(t_i)$ as:

$$\tilde{I}_m(t_i) = 0.25 \times [I_m(t_{i+1}) + 2I_m(t_i) + \tilde{I}_m(t_{i-1})] \quad (26)$$

where $\tilde{I}_m$ stands for the averaged currents whereas I_m stands for the currents without average. Although it is well known that the averaging scheme (26) is not possible to stabilize the MOT scheme for all cases, it seems to work well in this MOT scheme, and the later numerical examples show that the accuracy loss brought by this averaging scheme can be neglected.

3. 2-D TRANSIENT FAR SCATTERED FIELD

For the 2-D TM case, the scattered field may be expressed as:

$$\vec{E}(\vec{\rho},t) = -\frac{\partial \vec{A}(\vec{\rho},t)}{\partial t} \tag{27}$$

Using 2-D time-domain Green function, the magnetic vector potentials may be written as [31]:

$$\vec{A}(\vec{\rho},t) = \eta \int_C \int_0^{t-\tau} \frac{\vec{J}(\vec{\rho}',t')}{2\pi\sqrt{(ct-ct')^2 - |\vec{\rho}-\vec{\rho}'|^2}} dt' dC' \quad (t \geq \tau) \tag{28}$$

where η is the wave impedance of the surrounding medium, and $\vec{\rho}$ and $\vec{\rho}'$ are the field point and source point respectively and $\tau = |\vec{\rho} - \vec{\rho}'|/c$.

For far-field case, $|\vec{\rho}| \gg |\vec{\rho}'|$, and $|\vec{\rho} - \vec{\rho}'| \simeq \rho - \hat{\rho} \cdot \vec{\rho}'$, where $\hat{\rho}$ is the unit vector, and $\rho = |\vec{\rho}|$. Then Eq. (28) can be rewritten as:

$$\vec{A}(\vec{\rho},t) = \eta \int_C \int_0^{t-\tau} \frac{\vec{J}(\vec{\rho}',t')}{2\pi\sqrt{(ct-ct'+\rho-\hat{\rho}\cdot\vec{\rho}')(ct-ct'-\rho+\hat{\rho}\cdot\vec{\rho}')}} dt' dC' \quad \text{and } t \geq \tau \tag{29}$$

Also for far field case, ρ can be large enough to give

$$\rho \gg \hat{\rho} \cdot \vec{\rho}' \tag{30}$$

For numerical calculations, the maxim time step $t'_{\max}$ which can be computed is limited. So if ρ is large enough there must be

$$\rho \gg ct'_{\max} \tag{31}$$

Furthermore, in Eq. (29) the integral upper limit of t' is $t'_{\max} = t - |\vec{\rho} - \vec{\rho}'|/c$, which leads to

$$ct = \rho + ct'_{\max} - \hat{\rho} \cdot \vec{\rho}' \tag{32}$$

Dividing both sides of Eq. (32) by ρ gives

$$\frac{ct}{\rho} \approx 1 \tag{33}$$

Thus, the following equation may be derived, given by:

$$\frac{1}{ct - ct' + \rho - \hat{\rho} \cdot \vec{\rho}'} \approx \frac{1}{2\rho} \tag{34}$$

Substituting Eq. (34) into Eq. (29) gives:

$$\sqrt{\rho}\vec{A}_f(\vec{\rho}, t) = \frac{\eta}{2\sqrt{2}\pi} \int_C \int_0^{t-\tau} \frac{\vec{J}(\vec{\rho}', t')}{\sqrt{(ct - ct' - \rho + \hat{\rho} \cdot \vec{\rho}')}} dt' dC' \text{ and } t \geq \tau \tag{35}$$

where symbol f in $\vec{A}_f$ refers to far-field. Approximating the contour C into straight-line segments, Eq. (35) can be written as

$$\sqrt{\rho}\vec{A}_f(\vec{\rho}, t) = \frac{\eta}{2\sqrt{2}\pi} \sum_{n=1}^{N} \Delta l_n \int_0^{t-\tau} \frac{\vec{J}_n(t')}{\sqrt{(ct - ct' - \rho + \hat{\rho} \cdot \vec{\rho}_n')}} dt' \tag{36}$$

where Δl_n is the length of the nth straight-line segment, and $\vec{\rho}_n'$ represents the middle point of nth segment, and $\tau = |\vec{\rho} - \vec{\rho}'_n|/c$. Moreover, Eq. (36) can be carried out analytically on the assumption that the current in a segment does not vary with time:

$$\sqrt{\rho}\vec{A}_f(\vec{\rho}, t_i) = \frac{\mu}{2\sqrt{2}\pi} \sum_{n=1}^{N} \Delta l_n \sum_{k=1}^{i-\tau_n} -2\vec{J}_n(t_k)(\sqrt{a - ct_k} - \sqrt{a - ct_{k-1}}) \tag{37}$$

where $\tau_n = (\rho - \hat{\rho} \cdot \vec{\rho}_n)/c$ and $a = ct_i - \rho + \hat{\rho} \cdot \vec{\rho}_n'$. Finally, we rewrite Eq. (27) and replace the time derivative with a central difference as:

$$\sqrt{\rho}\vec{E}_f(\vec{\rho}, t) = -\sqrt{\rho}\frac{\partial \vec{A}_f(\vec{\rho}, t_i)}{\partial t} = -\sqrt{\rho}\frac{\vec{A}_f(\vec{\rho}, t_{i+1}) - \vec{A}_f(\vec{\rho}, t_{i-1})}{2\Delta t} \tag{38}$$

4. NUMERICAL EXAMPLES

In this section, two numerical examples are presented. Because the TDPO method is only valid in high frequency case, a TM modulated Gaussian plane wave is used, which is defined as [32]

$$\vec{E}^{inc}(\vec{\rho}, t) = -\vec{E}_0^{inc} \cos\left[2\pi f_0 \left(t - \frac{\vec{\rho} \cdot \hat{k}^{inc}}{c}\right)\right] \frac{4.0}{\sqrt{\pi}T} e^{-\left[\frac{4.0}{T}(ct - ct_0 - \vec{\rho} \cdot \hat{k}^{inc})\right]^2} \tag{39}$$

where $\hat{k}^{inc}$ is the unit vector in the direction of propagation of the incident wave, and f_0 is the modulation frequency. All results shown

here are obtained with $\vec{E}0^{\text{inc}} = \hat{z}120\pi$, $T = 4\,\text{LM}$, $ct_0 = 6\,\text{LM}$, $\hat{k} = -\hat{x}$, and $f_0 = 900\,\text{MHz}$.

We first consider a straight strip with a 90° bent strip on the right side of it. As shown in Fig. 3, the combinative cylinders are located symmetrically along the $\hat{y}$ axis, and the straight strip is divided into 100 segments, while the bent strip is divided into a total of 10 segments. In this case, the straight strip is modeled as TDPO region while the bent strip as TDIE region, and the time step is 0.015 LM. Fig. 5(a) shows the result of the current response at point A (the midpoint in the upper side of the bent strip) by our hybrid method, and the

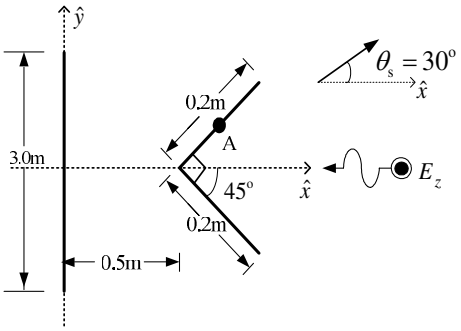

Figure 3. Combinative cylinders composed by straight strip and bent strip.

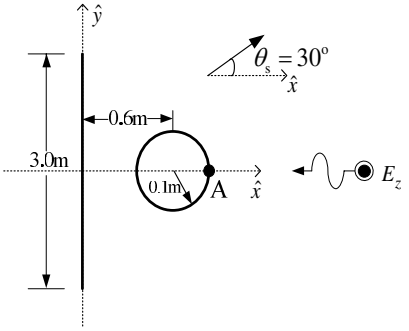

Figure 4. Combinative cylinders composed by straight strip and circular cylinder.

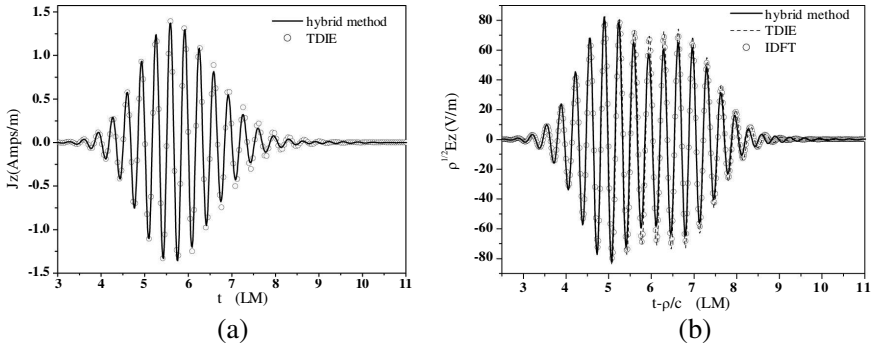

Figure 5. (a) Current response at the point A (refers to Fig. 3) illuminated by a TM modulated Gaussian plane wave. (b) Far scattered electric field response of combinative cylinders (refers to Fig. 3).

result is compared with that by TDIE. Fig. 5(b) shows the result of far scattered electric field response calculated by hybrid method with the scattering angle 30° from $\hat{x}$ axis ($\theta_s = 30°$), and this is compared with the results by TDIE and IDFT, respectively. It is easy for us to observe that the results by hybrid method agree well with those by TDIE in Figs. 5(a) and 5(b), but still some small discrepancies appear in later time. This is caused by the fact that TDPO is an asymptotic method, and the diffraction at edges is neglected here, while TDIE is a full wave method. As far as computing time is concerned, the ratio of TDIE and hybrid method is about 5 : 1 for each time step.

In addition, it is worthwhile to note that the results of far scattered electric field by TDIE are perfectly in accordance with those by IDFT in Fig. 5(b), which verifies the validity of the 2-D transient far-field computation method proposed in this paper.

As the second example, we consider the case of a straight strip with a circular cylinder on the right side of it, which is shown in Fig. 4. The combinative cylinders are also located symmetrically along the $\hat{y}$ axis. The straight strip is divided into 100 segments while the circular cylinder is divided into 20 segments. Similarly, the straight strip is modeled as TDPO region and the circular cylinder as TDIE region. The time step is 0.015 LM. Fig. 6(a) shows the results of the current response at point A by hybrid method and TDIE, respectively. Fig. 6(b) shows the results of the far scattered electric field response by hybrid method ($\theta_s = 30°$) which is compared with those by TDIE and IDFT, respectively. It is obvious that the conclusions gotten from Fig. 6 are the same as those in the previous numerical example. For

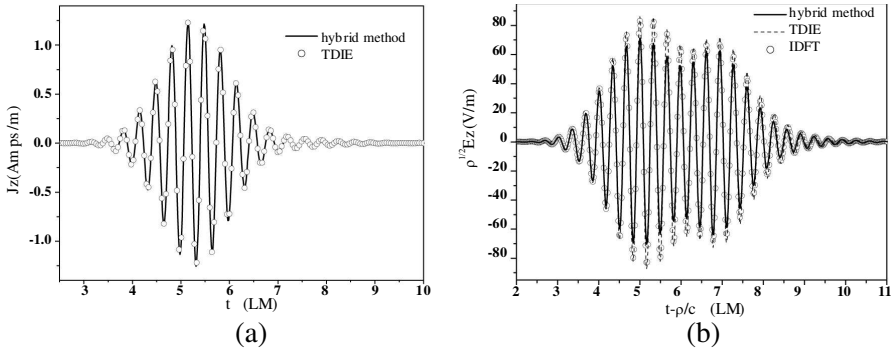

Figure 6. (a) Current response at the point A (refers to Fig. 4) illuminated by a TM modulated Gaussian plane wave. (b) The far scattered electric field response of combinative cylinders (refers to Fig. 4).

this numerical example, at each time step the ratio of the computing time of TDIE method and hybrid method is about 2.5 : 1.

5. CONCLUSION

A hybrid method which combines TDIE and TDPO is proposed for the problem of TM transient scattering from 2-D combinative conducting cylinders. The explicit solution procedure is developed in detail, and a concise time-domain near-zone to far-zone transformation algorithm without double Fourier transform is presented. Numerical results are compared with those obtain by TDIE and IDFT methods, and demonstrate the accuracy and high efficiency of our hybrid method, as well as the validity of 2-D transient near-zone to far-zone transformation algorithm.

ACKNOWLEDGMENT

This work was supported by the National Natural Science Foundation of China (NNSFC) (grant 60571058).

REFERENCES

1. Hatamzadeh-Varmazyar, S. and M. Naser-Moghadasi, "An integral equation modeling of electromagnetic scattering from the surfaces of a rbitrary resistance distribution," *Progress In Electromagnetics Research B*, Vol. 3, 157–172, 2008.
2. Zhuang, W., Z. Fan, D.-Z. Ding, and Y. An, "Fast analysis and design of frequency selective surface using the gmresr-FFT method," *Progress In Electromagnetics Research B*, Vol. 12, 63–80, 2009.
3. Fan, Z., D.-Z. Ding, and R.-S. Chen, "The efficient analysis of electromagnetic scattering from composite structures using hybrid CFIE-IEFIE," *Progress In Electromagnetics Research B*, Vol. 10, 131–143, 2008.
4. Danesfahani, R., S. Hatamzadeh-Varmazyar, E. Babolian, and Z. Masouri, "Applying shannon wavelet basis functions to the method of moments for evaluating the radar cross section of the conducting and resistive surfaces," *Progress In Electromagnetics Research B*, Vol. 8, 257–292, 2008.
5. Mittra, R. and K. Du, "Characteristic basis function method for iteration-free solution of large method of moments problems," *Progress In Electromagnetics Research B*, Vol. 6, 307–336, 2008.

6. Hassani, H. R. and M. Jahanbakht, "Method of moment analysis of finite phased array of aperture coupled circular microstrip patch antennas," *Progress In Electromagnetics Research B*, Vol. 4, 197–210, 2008.
7. Yuan, J., Y. Qiu, and Q. Z. Liu, "Fast analysis of multiple antennae coupling on very electrical large objects via parallel technique," *Journal of Electromagnetic Waves and Applications*, Vol. 22, No. 8–9, 1232–1241, 2008.
8. Engheta, N., W. D. Murphy, V. Rokhlin, et al., "The fast multipole method (FMM) for electromagnetic scattering problems," *IEEE Transactions on Antennas and Propagation*, Vol. 40, No. 6, 634–641, Jun. 1992.
9. Yuan, H. B., N. Wang, and C. H. Liang, "Fast algorithm to extract the singularity of higher order moment method," *Journal of Electromagnetic Waves and Applications*, Vol. 22, No. 8–9, 1250–1257, 2008.
10. Chen, Y., S. Yang, S. He, and Z.-P. Nie, "Design and analysis of wideband planar monopole antennas using the multilevel fast multipole algorithm," *Progress In Electromagnetics Research B*, Vol. 15, 95–112, 2009.
11. Su, D. Y., D.-M. Fu, and D. Yu, "Genetic algorithms and method of moments for the design of Pifas," *Progress In Electromagnetics Research Letters*, Vol. 1, 9–18, 2008.
12. Essid, C., M. B. B. Salah, K. Kochlef, A. Samet, and A. B. Kouki, "Spatial-spectral formulation of method of moment for rigorous analysis of microstrip structures," *Progress In Electromagnetics Research Letters*, Vol. 6, 17–26, 2009.
13. Balaban, M. V., R. Sauleau, T. M. Benson, and A. I. Nosich, "Dual integral equations technique in electromagnetic wave scattering by a thin disk," *Progress In Electromagnetics Research B*, Vol. 16, 107–126, 2009.
14. Huang, Y., Q. Z. Liu, Y. Zou, and L. Sun, "A hybrid FE-BI method for electromagnetic scattering from dielectric bodies partially covered by conductors," *Journal of Electromagnetic Waves and Applications*, Vol. 22, No. 2–3, 423–430, 2008.
15. Bayer, S. E. and A. A. A. Ergin, "A stable Marching-On-in-Time scheme for wire scatterers using a Newmark-Beta formulation," *Progress In Electromagnetics Research B*, Vol. 6, 337–360, 2008.
16. Rynne, B. P., "Time domain scattering from arbitrary surfaces using the electric field integral equation," *Journal of Electromagnetic Waves and Applications*, Vol. 5, No. 1, 93–112, Jan. 1991.

17. Rao, S. M. and D. R. Wilton, "Transient scattering by conducting surfaces of arbitrary shape," *IEEE Transactions on Antennas and Propagation*, Vol. 39, No. 1, Jan. 1991.
18. Dadvies, P. J., "Stability of time-marching numerical schemes for the electric field integral equation," *Journal of Electromagnetic Waves and Applications*, Vol. 8, No. 1, 85–114, Jan. 1994.
19. Rynne, B. P. and P. D. Smith, "Stability of time marching algorithms for the electric field integral equation," *Journal of Electromagnetic Waves and Applications*, Vol. 4, No. 12, 1181–1205, Dec. 1990.
20. Ergin, A. A., B. Shanker, and E. Michielssen, "The plane wave time-domain algorithm for the fast analysis of transient wave phenomena," *IEEE Antennas Propagat. Mag.*, Vol. 41, No. 4, 39–52, Sep. 1999.
21. Shanker, B., A. A. Ergin, K. Aygun, and E. Michielssen, "Analysis of transient electromagnetic scattering phenomena using a two-level plane wave time domain algorithm," *IEEE Transactions on Antennas and Propagation*, Vol. 48, No. 4, 510–523, 2000.
22. Shanker, B., A. A. Ergin, K. Aygun, and M. Y. Lu, "Fast analysis of transient electromagnetic scattering phenomena using the multilevel plane wave time domain algorithm," *IEEE Transactions on Antennas and Propagation*, Vol. 51, No. 3, Mar. 2003.
23. Walker, S. P. and M. J. Vartiainen, "Hybridization of curvilinear time-domain integral equation and time-domain optical methods for electromagnetic scattering analysis," *IEEE Transactions on Antennas and Propagation*, Vol. 46, No. 3, 318–324, 1998.
24. Ren, M., et al., "Coupled TDIE-PO method for transient scattering from electrically large conducting objects," *Electronics Letters*, Vol. 44, No. 4, 258–260, 2008.
25. Qin, Y., D. Zhou, J. He, and P. Liu, "A UTD enhanced PO-TDIE hybrid algorithm," *Progress In Electromagnetics Research M*, Vol. 8, 153–162, 2009.
26. Damaskos, N. J., et al., "Transient scattering by resistive cylinders," *IEEE Transactions on Antennas and Propagation*, Vol. 33, No. 1, 21–25, 1985.
27. Vechinski, D. A. and S. M. Rao, "Transient scattering by conducting cylinders-TE case," *IEEE Transactions on Antennas and Propagation*, Vol. 40, No. 9, 1103–1107, Sep. 1992.
28. Vechinski, D. A. and S. M. Rao, "Transient scattering from two-dimensional dielectric cylinders and arbitrary shape," *IEEE Transactions on Antennas and Propagation*, Vol. 40, No. 9, 1054–

1060, Sep. 1992.

29. Rao, S. M., *Time Domain Electromagnetic*, Ch. 3, Academic, 1999.
30. Luebbers, R. J., D. Ryan, and J. Beggs, "A two-dimensional time-domain near-zone to far-zone transformation," *IEEE Transactions on Antennas and Propagation*, Vol. 40, No. 7, 848–851, Jul. 1997.
31. Chew, W. C., *Waves and Fields in Inhomogeneous Media*, Ch. 4, IEEE Press, New York, 1995.
32. Carin, L. and L. B. Felsen, *Electromagnetics 2: Ultra-wideband Short-pulse*, 273–284, Plenum Press, New York, 1995.